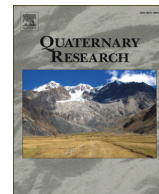




Contents lists available at ScienceDirect



## Quaternary Research

journal homepage: [www.elsevier.com/locate/yqres](http://www.elsevier.com/locate/yqres)

# Carbon and oxygen stable isotope compositions of late Pleistocene mammal teeth from dolines of Ajoie (Northwestern Switzerland)

Laureline Scherler <sup>a,b,\*</sup>, Thomas Tütken <sup>c</sup>, Damien Becker <sup>d</sup><sup>a</sup> Institut des Sciences de l'Evolution, Place Eugène Bataillon, Université de Montpellier 2, F-34095 Montpellier, France<sup>b</sup> Paléontologie A16, Office de la Culture, République et Canton du Jura, Hôtel des Halles, CH-2900 Porrentruy, Switzerland<sup>c</sup> Institut für Geowissenschaften, AG für Angewandte und Analytische Paläontologie, Johannes Gutenberg-Universität Mainz, J.-J.-Becher-Weg 21, D-55099 Mainz, Germany<sup>d</sup> JURASSICA Muséum, Route de Fontenais 21, CH-2900 Porrentruy, Switzerland

## ARTICLE INFO

## Article history:

Received 8 October 2013

Available online xxxx

## Keywords:

Megaherbivores

Tooth enamel

Early Glacial

Middle Pleniglacial

Paleoenvironment

Paleoclimate

Paleodiet

## ABSTRACT

Fossils of megaherbivores from eight late Pleistocene  $^{14}\text{C}$ - and OSL-dated doline infillings of Ajoie (NW Switzerland) were discovered along the Transjurane highway in the Swiss Jura. Carbon and oxygen analyses of enamel were performed on forty-six teeth of large mammals (*Equus germanicus*, *Mammuthus primigenius*, *Coelodonta antiquitatis*, and *Bison priscus*), coming from one doline in Boncourt (~80 ka, marine oxygen isotope stage MIS5a) and seven in Courtedoux (51–27 ka, late MIS3), in order to reconstruct the paleoclimatic and paleoenvironmental conditions of the region. Similar enamel  $\delta^{13}\text{C}$  values for both periods, ranging from  $-14.5$  to  $-9.2\text{\textperthousand}$ , indicate that the megaherbivores lived in a  $C_3$  plant-dominated environment. Enamel  $\delta^{18}\text{O}_{\text{PO}_4}$  values range from  $10.9$  to  $16.3\text{\textperthousand}$  with a mean of  $13.5 \pm 1.0\text{\textperthousand}$  ( $n = 46$ ). Mean air temperatures (MATs) were inferred using species-specific  $\delta^{18}\text{O}_{\text{PO}_4}$ – $\delta^{18}\text{O}_{\text{H}_2\text{O}}$ -calibrations for modern mammals and a present-day precipitation  $\delta^{18}\text{O}_{\text{H}_2\text{O}}$ -MAT relation for Switzerland. Similar average MATs of  $6.6 \pm 3.6^\circ\text{C}$  for the deposits dated to ~80 ka and  $6.5 \pm 3.3^\circ\text{C}$  for those dated to the interval 51–27 ka were estimated. This suggests that these mammals in the Ajoie area lived in mild periods of the late Pleistocene with MATs only about  $2.5^\circ\text{C}$  lower than modern-day temperatures.

© 2014 University of Washington. Published by Elsevier Inc. All rights reserved.

## Introduction

Climate conditions are reflected in the taxonomic composition of the mammal faunas (e.g., Brugal and Croitor, 2007), as well as in the oxygen isotope composition of mammalian bones and teeth (e.g., Koch, 1998). Therefore, Pleistocene mammal assemblages are of special interest for paleoclimatic reconstruction, as Quaternary climates repeatedly shifted from cold to warm temperatures over short periods of time (Zachos et al., 2001). The Middle Pleniglacial (Marine Oxygen Isotope Stage (MIS) 3) usually considered as a mega-interstadial with several warmer and cooler intervals (Van Andel and Davies, 2003), was the warmest part of the Weichselian (~115 to 11.7 ka; MIS5 to MIS2). According to data obtained from Western Europe, the final part of MIS3 corresponds to the Hengelo, Huneborg and Denekamp interstadials ("glacial interstadials" GI11 to GI5), which roughly preceded the Last Glacial Maximum of the Late Pleniglacial (Johnsen et al., 1997; Markova et al., 2009). These interstadials are typically recorded in the sequence of infillings of the dolines in Ajoie (NW Switzerland), comprising many fossils of large mammals from the so-called Mammoth Steppe fauna

(or the late Pleistocene *Mammuthus*–*Coelodonta* faunal complex; Kahlke, 1999). These fossils yield important information about environmental and climatic conditions of this time interval, even though minor climatic changes such as interstadials did not drastically change the faunal composition. The interval GI11 to GI5 coincided with the extinction of *Homo neanderthalensis* and the spread of *Homo sapiens* in Europe (Johnson, 2002; Van Andel and Davies, 2003; Mellars, 2004; Manzi, 2011). However, the Mammoth Steppe fauna remained unaltered after the arrival of anatomically modern humans until the beginning of the Last Glacial Maximum, when these megaherbivores vanished (von Koenigswald, 2006).

Eight late Pleistocene doline infillings were excavated along the Transjurane highway in Ajoie, near Porrentruy (Canton Jura, NW Switzerland). Skeletal remains of late Pleistocene mammals were found in fossiliferous layers alongside with gastropods and charcoal. Radiocarbon dating of these mammal bones, gastropod shells (*Arianta arbustorum*), and charcoal, as well as OSL (optically stimulated luminescence) analyses of the embedding sediments were performed to constrain the timing of doline formation (Becker et al., 2013). Two phases of doline infillings with late Pleistocene mammal fossils were detected: a latest Early Glacial filling phase within the doline from Boncourt-Grand Combe (GC) and a late Middle Pleniglacial filling phase within the seven dolines from Courtedoux-Vâ Tche Tchâ (VTA-SY, -V1, -V2,

\* Corresponding author.

E-mail addresses: laureline.scherler@net2000.ch (L. Scherler), tuetken@uni-mainz.de (T. Tütken), damien.becker@jura.ch (D. Becker).

-V3, -V4, -V6, and -V14). The skeletal remains represent a typical late Pleistocene mammalian fauna adapted to cold climate with *Mammuthus primigenius* (Proboscidea), *Equus germanicus* and *Coelodonta antiquitatis* (Perissodactyla), and *Bison priscus* (Artiodactyla). Forty-six teeth of these large mammals were analysed for their enamel carbon ( $\delta^{13}\text{C}$ ) and oxygen ( $\delta^{18}\text{O}_{\text{CO}_3}$  and  $\delta^{18}\text{O}_{\text{PO}_4}$ ) isotopic compositions in order to characterise the paleodiets of these megaherbivores and to reconstruct the paleoclimatic and paleoenvironmental conditions in Ajoie during the mild periods of the latest Early Glacial and the late Middle Pleniglacial.

#### Geological setting and age of the dolines

The Ajoie region is located in NW Switzerland and belongs to the Tabular Jura (Fig. 1). Boarded northwards by the Sundgau plain (the southern extension of the Rhine Graben) and southwards by the Folded Jura, it was affected first by the Oligocene E-W extension phase that led to the opening of the Rhine and Bresse Grabens, then by the N-S compression phase that erected the Jura Mountains during the terminal Miocene. The Bure Plateau, on which the investigated dolines are situated, forms a vast horst located in Western Ajoie. It is characterised by a classical karstic geomorphology of the Kimmeridgian calcareous basement inherited from the late Pleistocene periglacial context. This landscape is essentially formed by dry valleys and dolines clogged by Pleniglacial to Late Glacial fluvial gravels and loess (e.g., Braillard, 2006; Becker et al., 2009). Regarding the local Quaternary record (Fig. 2), a reference stratigraphy of the Late Pleistocene and the Holocene was established with the Mousterian site of Alle-Noir Bois (Aubry et al., 2000). Recently, Braillard (2006, 2009) determined the local chrono-lithostratigraphic sequence on the base of the Quaternary deposits within the dry valleys, allowing good correlations with the

Weichselian loess series recorded within the Rhine Graben (Antoine et al., 2001). In contrast, the sediments of the Ajoie doline infillings are highly disturbed, mainly due to continuous interactions between deposition, transport, and erosion. The doline infillings of GC and VTA formed in a dry valley (oriented NNW–SSE) that cut the Kimmeridgian limestones and marls of the Reuchenette Formation (Gygi, 2000). As illustrated in Figure 2, the sedimentary sequence recorded within these dolines can be subdivided in eight chrono-lithostratigraphic units (D8–1), following an analogous nomenclature to that already proposed for this region (e.g., Aubry et al., 2000; Guélat, 2005; Braillard, 2009). The base of the infilling sequence, which is not always preserved, is constituted by loessic lenses trapped within a clayey matrix of gravels (D8). Most of the infillings are formed by gravel and loessic deposits, products of solifluction, debris flows, and sediment runoff (D7–5). Silty colluvium (D4), probably of loessic origin, can also be preserved at the top of the sequence, which is covered by Holocene humus-bearing deposits (D3–1).

All mammal teeth analysed in this study, from the single doline of GC and from the seven infillings of VTA, were collected in loessic beds of gravels that correspond to the chrono-lithostratigraphic units D8 and D6, respectively. Based on four OSL analyses made on the sediment of the VTA-V6, -SY, and GC dolines, the unit D8 is dated to the interval 121.3 to 67.0 ka (Early Glacial; Table 1). However, if the sediment strictly associated to the mammalian remains of GC is solely considered, the OSL analyses yield an age of  $78.0 \pm 11.0$  ka (latest Early Glacial). Radiocarbon analyses made on shells (*A. arbustorum* var. *alpicola*; Becker et al., 2013), charcoal and one mammoth bone from the unit D6 of the VTA dolines yield a late Middle Pleniglacial age, corresponding to the chronostratigraphic interval 44.0 to 34.5 cal ka BP (Table 2), whereas the OSL dating covers the interval 51.3 to 27.4 ka (Table 1). Radiocarbon dating of a *M. primigenius* bone from VTA-SY gave a

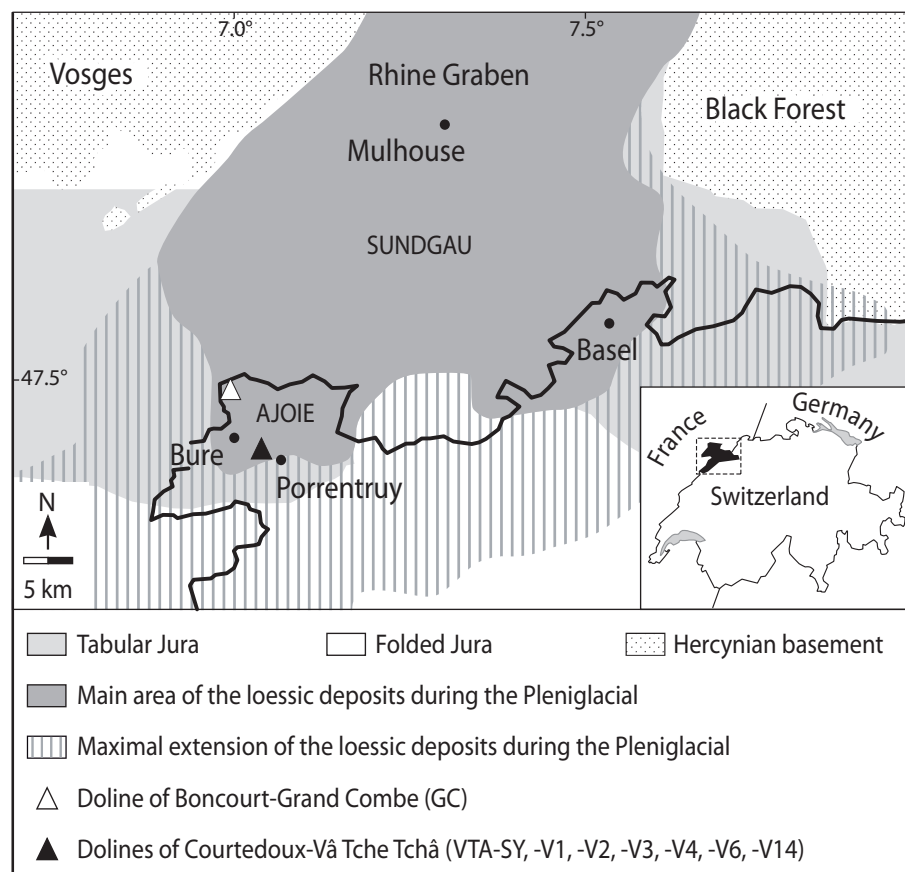


**Figure 1.** Geographical and geological setting of the doline infillings from Boncourt-Grand Combe (GC) and Courtedoux-Vâ Tche Tchâ (VTA) in Ajoie (NW Switzerland; modified from Becker et al., 2013).

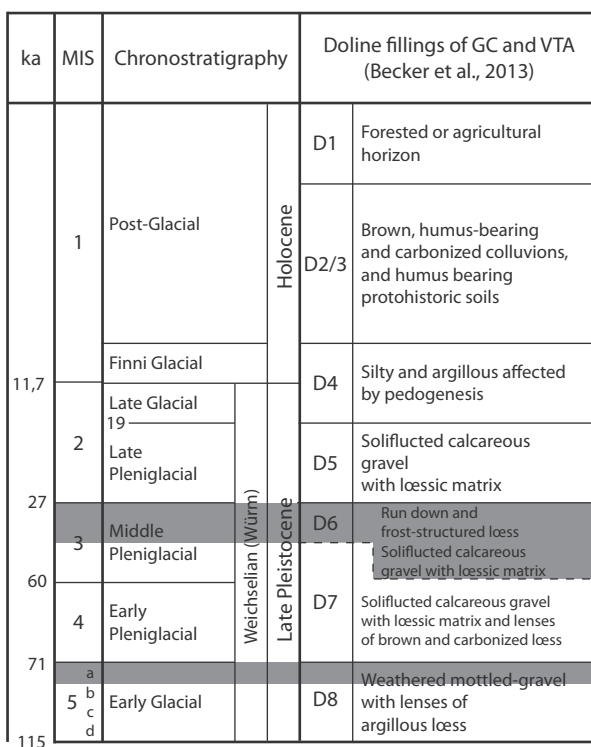


**Figure 2.** Synthetic chrono- and lithostratigraphy of the late Pleistocene and Holocene deposits recorded in Ajoie (NW Switzerland; modified from Becker et al., 2013); chronostratigraphy according to Haq (2007); Marine Oxygen Isotope Stage (MIS) according to Bassinot et al. (1994), except for MIS3, which is according to Svensson et al. (2006) and Van Meerbeeck et al. (2009). GC: doline of Boncourt-Grand Combe; VTA: dolines of Courtedoux-Vâ Tche Tchâ; grey areas: occurrence of mammal remains.

calibrated age of  $36.5 \pm 1.5$  cal ka BP (Table 2). Based on these results, we assume a latest Early Glacial age ( $\sim 80$  ka) for the analysed mammal specimens of the GC doline filling, and a late Middle Pleniglacial age (51–27 ka) for those from VTA.

#### Carbon and oxygen stable isotopes as proxies for diet and climate

Carbon and oxygen isotopes of mammalian skeletal bioapatite are well-established proxies for the reconstruction of paleodiets and paleoenvironmental conditions (e.g., Koch, 1998, 2007; Kohn and Cerling, 2002). Carbon isotopes in the carbonate moiety of bioapatite of herbivores are related to the  $\delta^{13}\text{C}$  values of the ingested plants. These are mainly controlled by the photosynthetic pathway, but can be additionally influenced by environmental factors such as humidity and vegetation density (O'Leary, 1988; Farquhar et al., 1989; Van der

Merwe and Medina, 1991; Heaton, 1999). The two main photosynthetic pathways are the Calvin cycle (or C<sub>3</sub> pathway; used by trees, shrubs, herbs, and cool-season grasses and sedges) and the Hatch–Slack cycle (or C<sub>4</sub> pathway; used by warm-season grasses and sedges). Their respective  $\delta^{13}\text{C}$  values range from  $-35$  to  $-23\text{\textperthousand}$  for the C<sub>3</sub> plants and from  $-14$  to  $-10\text{\textperthousand}$  for the C<sub>4</sub> plants (e.g., O'Leary, 1988; Farquhar et al., 1989). Herbivorous mammals record the  $\delta^{13}\text{C}$  values of ingested plants in their tissues (tooth enamel, bone collagen, hair, etc.) with a specific isotopic shift of  $14.1 \pm 0.5\text{\textperthousand}$  for tooth enamel of large ungulate mammals (Cerling and Harris, 1999). Today, pure C<sub>3</sub>-plant feeders will have tooth enamel  $\delta^{13}\text{C}$  values lower than  $-8\text{\textperthousand}$  with average values of around  $-12.5\text{\textperthousand}$ , whereas C<sub>4</sub>-plant feeders will provide values higher than  $0\text{\textperthousand}$  (e.g., Cerling et al., 1997; Koch, 1998). Additionally, tooth enamel  $\delta^{13}\text{C}$  values within a pure C<sub>3</sub>-plant ecosystem may highlight niche partitioning or characterise the vegetation cover (e.g., Cerling et al., 2004; Feranec and MacFadden, 2006; Feranec, 2007; Tütken and Vennemann, 2009).

The phosphate  $\delta^{18}\text{O}$  values ( $\delta^{18}\text{O}_{\text{PO}_4}$ ) of biogenic bone or tooth apatite of vertebrates are preferentially used for reconstructing terrestrial paleoclimatic conditions (e.g., Longinelli, 1984; Bryant et al., 1996; Fricke and O'Neil, 1996; Fricke et al., 1998). This is because the  $\delta^{18}\text{O}$  value of the body water pool is determined by the oxygen inputs in the body, such as liquid water, atmospheric O<sub>2</sub>, and oxygen in food (e.g., Bryant and Froelich, 1995; Kohn, 1996). Due to constant mammalian body temperatures, and thus a constant oxygen isotope fractionation,  $\delta^{18}\text{O}$  values of environmental water, body water, and skeletal apatite of bones and teeth of mammals are linearly related and oxygen isotopic composition of body water reflects that of meteoric water ingested by the animals (Longinelli, 1984). The  $\delta^{18}\text{O}_{\text{H}_2\text{O}}$  values of meteoric water are controlled by fractionation processes during the atmospheric water cycle and water vapour transport, and, especially at mid- and high-latitudes, air temperature and humidity during precipitation are the major controlling factors (Dansgaard, 1964; Rozanski et al., 1993; Fricke and O'Neil, 1999). Bioapatite  $\delta^{18}\text{O}$  values of water-dependent, obligate drinking mammals record best meteoric water values and, hence, climatic conditions (Longinelli, 1984; Kohn, 1996; Levin et al., 2006).

#### Material and methods

##### Fossil mammal teeth

Forty-six teeth of large mammals from eight doline infillings of the Ajoie area (Fig. 1) were sampled for stable isotope analysis. One doline is located in Boncourt-Grand Combe (GC; unit D8,  $\sim 80$  ka) and the seven others in Courtedoux-Vâ Tche Tchâ (VTA-SY, -V1, -V2, -V3, -V4, -V6, and -V14; unit D6, 51–27 ka). Eight teeth come from GC and 38 from VTA (Table 3). Enamel samples were taken from ten teeth of *M. primigenius* (Elephantidae), seventeen of *E. germanicus* (Equidae), eleven of *C. antiquitatis* (Rhinocerotidae), and eight of *B. priscus* (Bovidae), determined by Rothen et al. (2011), Savoy et al. (2012) and DB and LS (pers. obs.). None of these isolated and/or fragmentary teeth could be associated, so each fossil probably belonged to a different individual. They are housed in the Musée jurassien des sciences naturelles (MJSN; Porrentruy, Switzerland).

##### Analytical methods for stable isotopes

Tooth enamel was sampled using a diamond-studded microdrill of 0.8 mm diameter and 10 mg of powder were removed drilling a single transect along the direction of growth of the crown, comprising 50–90% of crown height for most teeth (Table 3). Enamel was first pre-cleaned and then carefully sampled avoiding any dentine contamination. All analysed powders were white and no traces of leaching or root marks were observed on the fossils. The enamel powders were pre-treated with 2% NaOCl and 0.1 M acetic acid according to the

**Table 1**  
OSL ages (ka) for the doline fillings of Boncourt-Grand Combe (GC) and Courtedoux-Vâ Tche Tchâ (VTA).

Doline	Laboratory number	OSL age (ka)	Unit	MIS
VTA-SY	C-L1051	$33.2 \pm 5.8$	D6	3
VTA-V6	L2196	$38.3 \pm 7.0$	D6	3
VTA-V14	L2190	$38.6 \pm 7.1$	D6	3
VTA-V2	L2198	$42.8 \pm 5.5$	D6	3
VTA-V6	L2194	$42.9 \pm 5.3$	D6	3
VTA-V6	L2195	$44.3 \pm 7.0$	D6	3
VTA-V14	L2189	$50.9 \pm 6.4$	D7	3
VTA-SY	C-L1049	$64.9 \pm 20.1$	D7	3
GC	C-L1397	$65.0 \pm 9.0$	D7	4
GC	C-L1398	$78.0 \pm 11.0$	D8	5a
VTA-V6	L2192	$82.5 \pm 11.9$	D8	5a
VTA-V6	L2191	$93.7 \pm 14.2$	D8	5b
VTA-SY	C-L1050	$100.6 \pm 20.7$	D8	5c

**Table 2**

Radiocarbon ( $^{14}\text{C}$  ka BP) and calibrated ages (cal ka BP) for the doline fillings of Courtedoux-Vâ Tche Tchâ (VTA). Calibrated ages according to <http://www.calpal-online.de>.

Doline	Laboratory number	$^{14}\text{C}$ age ( $^{14}\text{C}$ ka BP)	Calibr. age (cal ka BP)	Unit	MIS
VTA-SY	Ua-16438 (bone)	31.595 ± 1.335	34.5–37.5	D6	3
VTA-V1	Ua-36664 (charcoal)	33.360 ± 1.120	36.5–39.0	D6	3
VTA-V2	Ua-33122 (shell)	33.045 ± 0.830	37.0–39.5	D6	3
VTA-V1	Ua-36668 (shell)	37.015 ± 1.360	40.0–43.0	D6	3
VTA-V2	Ua-33123 (shell)	37.890 ± 1.515	41.0–44.0	D6	3

method established by Koch et al. (1997) for analysing the structural carbonate and phosphate of the apatite. Around 1.5 mg pre-treated powder was analysed using a ThermoFinnigan Gasbench II coupled to a Finnigan Delta Plus XL continuous-flow isotope ratio gas mass spectrometer in the stable isotope laboratory of the University of Tübingen (Germany), for the carbon ( $\delta^{13}\text{C}$ ) and oxygen ( $\delta^{18}\text{O}_{\text{CO}_3}$ ) isotopic composition of the structural carbonate in the apatite with a precision of better than  $\pm 0.1\text{\textperthousand}$  and  $0.17\text{\textperthousand}$ , respectively. For  $\delta^{18}\text{O}_{\text{PO}_4}$  analyses, 4 mg aliquots of the pre-treated enamel powder were dissolved in 2 M HF and after neutralisation with 25% ammonia solution, the  $\text{PO}_4^{3-}$  ions were rapidly precipitated as  $\text{Ag}_3\text{PO}_4$  by the addition of 2 N silver nitrate solution according to the protocol established by Tütken et al. (2006). Around 500 µg of  $\text{Ag}_3\text{PO}_4$  were weighted in silver capsules and analysed in triplicate using a ThermoFinnigan TC/EA coupled to a Finnigan Delta Plus XL continuous-flow isotope ratio gas mass spectrometer with a precision of better than  $\pm 0.3\text{\textperthousand}$ , in the same laboratory.

Isotopic compositions are expressed in the delta notation and reported as ‰-deviation relative to the Vienna PeeDee belemnite (VPDB) scale for the  $\delta^{13}\text{C}$  and  $\delta^{18}\text{O}_{\text{CO}_3}$  values, and relative to the Vienna Standard Mean Ocean Water (VSMOW) scale for the  $\delta^{18}\text{O}_{\text{PO}_4}$  values. The  $\delta^{18}\text{O}_{\text{CO}_3}$  VPDB values were recalculated to the VSMOW scale using the equation:  $\delta^{18}\text{O}_{\text{VSMOW}} = 1.03091 \times \delta^{18}\text{O}_{\text{VPDB}} + 30.91$  (Coplen et al., 1983). For quality control, the international phosphate standard NIST SRM 120c was analysed with the same protocol yielding  $\delta^{18}\text{O}_{\text{CO}_3}$  and  $\delta^{13}\text{C}$  values of  $-6.31 \pm 0.04\text{\textperthousand}$  and  $-1.79 \pm 0.17\text{\textperthousand}$  ( $n = 4$ ), respectively, and a  $\delta^{18}\text{O}_{\text{PO}_4}$  value of  $21.4 \pm 0.1\text{\textperthousand}$  ( $n = 3$ ).

## Results

The results of the carbon ( $\delta^{13}\text{C}$ ) and oxygen ( $\delta^{18}\text{O}_{\text{CO}_3}$  and  $\delta^{18}\text{O}_{\text{PO}_4}$ ) isotopic compositions of tooth enamel of the megaherbivores from VTA and GC are given in Table 3, along with the calculated  $\delta^{18}\text{O}_{\text{H}_2\text{O}}$  values and paleotemperatures (in °C). Table 4 synthesises the mean values for each taxon. Figure 3A–D illustrates the  $\delta^{13}\text{C}$  and  $\delta^{18}\text{O}_{\text{PO}_4}$  values of the four different taxa from both time period (GC, ~80 ka, and VTA, 51–27 ka).

### $\delta^{13}\text{C}_{\text{VPDB}}$ values

The  $\delta^{13}\text{C}$  values of all analysed teeth from the doline of GC average  $-11.5 \pm 0.6\text{\textperthousand}$  ( $n = 8$ ), with the lowest  $\delta^{13}\text{C}$  value for the single tooth of *M. primigenius* ( $-12.6\text{\textperthousand}$ ) and the highest for the single tooth of *B. priscus* ( $-10.5\text{\textperthousand}$ ).

The mean  $\delta^{13}\text{C}$  value of the analysed teeth from the seven doline infillings of VTA is  $-11.6 \pm 0.9\text{\textperthousand}$  ( $n = 38$ ), which is similar to the mean value from the GC specimens. The lowest intra-specific mean is displayed by the mammoths ( $-12.1 \pm 0.4\text{\textperthousand}$ ,  $n = 9$ ), but the lowest  $\delta^{13}\text{C}$  value is recorded in an M1 of *B. priscus* ( $-14.5\text{\textperthousand}$ ). The highest mean value is displayed by the rhinoceroses ( $-11.2 \pm 0.3\text{\textperthousand}$ ,  $n = 7$ ), and the highest  $\delta^{13}\text{C}$  value is recorded in a fragmentary tooth of *E. germanicus* ( $-9.2\text{\textperthousand}$ ). Concerning the intra-specific variation, the bison teeth display the highest standard deviation ( $1.5\text{\textperthousand}$ ,  $n = 7$ ) and the rhinoceroses the lowest ( $0.3\text{\textperthousand}$ ,  $n = 7$ ).

### $\delta^{18}\text{O}$ values

The  $\delta^{18}\text{O}_{\text{CO}_3}$  vsmow and  $\delta^{18}\text{O}_{\text{PO}_4}$  vsmow values seem to be in isotopic equilibrium for the majority of enamel samples (Fig. 4), as most of them plot in the prediction interval expected for modern vertebrates (Pellegrini et al., 2011). However, three enamel samples seem to be diagenetically altered, as they plot well below the equilibrium range towards higher  $\delta^{18}\text{O}_{\text{CO}_3}$  values. For this reason, the results of the  $\delta^{18}\text{O}_{\text{CO}_3}$  values are only given in the database (Table 3) and only the  $\delta^{18}\text{O}_{\text{PO}_4}$  values are discussed.

The  $\delta^{18}\text{O}_{\text{PO}_4}$  values of all analysed teeth from the doline of GC average  $13.6 \pm 1.1\text{\textperthousand}$  ( $n = 8$ ), with the lowest  $\delta^{18}\text{O}_{\text{PO}_4}$  value for a horse M2 ( $11.9\text{\textperthousand}$ ) and the highest for the single bison upper molar ( $14.8\text{\textperthousand}$ ).

The mean  $\delta^{18}\text{O}_{\text{PO}_4}$  value of the analysed teeth from the infillings of VTA averages  $13.5 \pm 1.1\text{\textperthousand}$  ( $n = 38$ ), which is similar to the mean from GC. The lowest intra-specific mean is displayed by the horses ( $13.1 \pm 0.9\text{\textperthousand}$ ,  $n = 15$ ), the highest mean by the bison ( $14.4 \pm 1.2\text{\textperthousand}$ ,  $n = 7$ ). The lowest and highest  $\delta^{18}\text{O}_{\text{PO}_4}$  values are recorded in a rhino P2 ( $10.9\text{\textperthousand}$ ) and a bison upper molar ( $16.3\text{\textperthousand}$ ), respectively. Additionally, the rhinos show the highest standard deviation ( $1.3\text{\textperthousand}$ ,  $n = 7$ ) and the horses and mammoths the lowest ( $0.86\text{\textperthousand}$ ,  $n = 15$  and  $0.88\text{\textperthousand}$ ,  $n = 9$ , respectively).

## Discussion

### Carbon isotopic composition

The seven dolines from Vâ Tche Tchâ are of similar age and lie very close to each other (within 500 m of maximal distance; Fig. 1). Therefore, the fauna of the fossil-bearing sediments should be more or less sympatric and the sampled enamel of megaherbivores is expected to display similar isotopic compositions. The mean enamel  $\delta^{13}\text{C}$  values for the older fauna of Grand Combe ( $-11.5 \pm 0.6\text{\textperthousand}$ ,  $n = 8$ ) are indistinguishable from those of VTA ( $-11.6 \pm 0.9\text{\textperthousand}$ ,  $n = 38$ ). These  $\delta^{13}\text{C}$  values indicate that the megaherbivores fed exclusively on a C<sub>3</sub>-plant diet. Since  $\delta^{13}\text{C}$  values of C<sub>3</sub> plants can be significantly influenced by environmental factors (Heaton, 1999; Diefendorf et al., 2010; Kohn, 2010), the environmental and climatic conditions were probably not very different during both time intervals. A relatively humid and open landscape partially covered by bushes, shrubs and trees developed under temperate climatic conditions (Becker et al., 2009, 2013). This mosaic or tundra-steppe habitat was confirmed by the presence of the northern birch mice (Oppliger and Becker, 2010).

The megaherbivores of the VTA doline infillings show small inter-specific variations in their carbon isotopic compositions (Fig. 3C). These subtle isotopic distinctions may though reflect a certain niche partitioning within this C<sub>3</sub>-plant ecosystem in the surrounding of the dolines, or may be due to discrepancies in digestive physiology or feeding behaviour. Indeed, bovids are foregut fermenters in contrast to rhinoceroses, horses, and mammoths, which are hindgut fermenters. Foregut fermenters usually produce and loose a larger fraction of isotopically light, <sup>13</sup>C-depleted methane during digestion (Passey et al., 2005). This implies that cows have a larger carbon isotope fractionation factor (14.6‰) between diet and skeletal apatite than hindgut

**Table 3**  
Carbon ( $\delta^{13}\text{C}$ ) and oxygen ( $\delta^{18}\text{O}_{\text{CO}_3}$  and  $\delta^{18}\text{O}_{\text{PO}_4}$ ) isotopic values of the analysed tooth enamel from the megaherbivores of Boncourt-Grand Combe (GC) and Courtedoux-Vâ Tche Tchâ (VTA), along with the calculated  $\delta^{18}\text{O}_{\text{H}_2\text{O}}$  values and estimated paleotemperatures ( $T^\circ\text{C}$ ). \*shows the calculated  $\delta^{18}\text{O}_{\text{H}_2\text{O}}$  values based on the general calibration equation for mammals as comparison, with the associated calculated temperatures (\*\*); values are shown in italics. Note that there is currently no species-specific calibration equation for rhinoceroses. Anatomical abbreviations of the teeth: d/D, lower/upper deciduous tooth; p/P, lower/upper premolar; m/M, lower upper molar.

Chemical number	Doline	Age (ka)	Tooth	Crown height (mm)	Sampling height (mm)	Crown sampled (%)	$\delta^{13}\text{C}$ VPDB (‰)	$\sigma$	$\delta^{18}\text{O}_{\text{CO}_3}$ VPDB (‰)	$\sigma$	$\delta^{18}\text{O}_{\text{CO}_3}$ VSMOW (‰)	$\delta^{18}\text{O}_{\text{PO}_4}$ VSMOW (‰)	$\sigma$	Wt% CaCO <sub>3</sub>	n	$\delta^{18}\text{O}_{\text{H}_2\text{O}}$ (‰)	*	T (°C)	**
<i>Mammuthus primigenius</i>																			
FT Ma SY/99 1	VTA SY	51–27	m2	–	27.0	–	–11.7	0.08	–9.0	0.09	21.6	11.6	0.3	6.4	1	–12.45	–13.56	3.96	1.42
FT Ma VTA/6 1	VTA V2	51–27	m1	71.0	45.0	63.38	–11.6	0.07	–8.7	0.06	21.9	13.7	0.3	6.8	2	–10.21	–11.23	9.04	6.72
FT Ma VTA/6 2	VTA V2	51–27	m3?	90.0	70.0	77.78	–12.0	0.03	–9.3	0.09	21.4	13.2	0.3	7.7	2	–10.74	–11.79	7.83	5.46
FT Ma VTA/6 3	VTA V2	51–27	m1	–	–	–	–12.5	0.08	–7.8	0.09	22.9	13.8	0.3	5.4	2	–10.11	–11.12	9.28	6.97
FT Mm VTA/06 3	VTA V2	51–27	–	49.0	26.0	53.06	–12.5	0.13	–7.2	0.17	23.5	14.8	0.0	5.0	2	–9.04	–10.01	11.70	9.50
FT Mm VTA/06 4	VTA V2	51–27	d/D?	95.0	20.0	21.05	–12.2	0.13	–7.4	0.13	23.3	14.1	0.3	4.7	1	–9.79	–10.79	10.01	7.73
FT Mm VTA/06 5	VTA V2	51–27	M1	91.0	76.0	83.52	–12.0	0.04	–7.9	0.07	22.8	13.7	0.3	6.8	2	–10.21	–11.23	9.04	6.72
FT Mm VTA/06 6	VTA V2	51–27	M2	102.0	13.0	12.75	–12.9	0.14	–8.6	0.21	22.0	13.7	0.0	5.1	2	–10.21	–11.23	9.04	6.72
FT Mm CTD/99 3	VTA V4	51–27	–	61.0	–	–	–11.7	0.16	–6.7	0.30	24.0	14.1	0.1	0.6	2	–9.79	–10.79	10.01	7.73
FT Mm BON/02 8	GC	~80	m2	27.0	11.0	40.74	–12.6	0.08	–7.1	0.06	23.6	14.7	0.3	4.2	1	–9.15	–10.12	11.46	9.24
<i>Equus germanicus</i>																			
FT Eq CTD/00 1	VTA SY	51–27	p/m	51.0	43.0	84.31	–11.7	0.09	–7.2	0.13	23.5	14.9	0.1	5.0	2	–10.00	–9.90	9.52	9.75
FT Eq CTD/00 2	VTA SY	51–27	p4?	62.0	33.0	53.23	–13.1	0.06	–7.5	0.16	23.2	13.4	0.5	4.2	2	–11.95	–11.57	5.10	5.96
FT Eq VTA/06 1	VTA V2	51–27	–	25.0	–	–11.4	0.05	–8.6	0.11	22.1	13.2	0.1	4.6	2	–12.21	–11.79	4.51	5.46	
FT Ma VTA/6 4	VTA V2	51–27	p2	56.0	39.0	69.64	–12.4	0.02	–9.6	0.03	21.0	13.6	0.3	7.4	2	–11.69	–11.34	5.69	6.47
FT Eq CTD/99 1	VTA V3	51–27	–	52.0	32.0	61.54	–12.4	0.06	–7.4	0.05	23.2	13.4	0.2	6.1	2	–11.95	–11.57	5.10	5.96
FT Eq CTD/99 2	VTA V3	51–27	d4	36.0	21.0	58.33	–12.6	0.07	–7.5	0.08	23.1	11.3	0.3	5.0	1	–14.68	–13.90	–1.10	0.67
FT Eq VTA/07 1	VTA V6	51–27	m3	67.0	37.0	55.22	–11.9	0.06	–9.2	0.13	21.5	12.7	0.3	5.8	1	–12.86	–12.34	3.03	4.20
FT Eq VTA/07 2	VTA V6	51–27	–	35.0	24.0	68.57	–11.8	0.12	–6.9	0.10	23.8	14.4	0.3	4.6	1	–10.65	–10.46	8.05	8.49
FT Eq VTA/07 3	VTA V6	51–27	P2	63.0	32.0	50.79	–11.7	0.11	–8.8	0.11	21.8	12.2	0.3	5.4	1	–13.51	–12.90	1.55	2.94
FT Eq VTA/07 4	VTA V6	51–27	–	32.0	19.0	59.38	–11.9	0.10	–8.4	0.12	22.2	13.2	0.3	4.7	1	–12.21	–11.79	4.51	5.46
FT Eq VTA/07 6	VTA V6	51–27	M1/2	24.0	12.0	50.00	–10.7	0.08	–8.6	0.12	22.0	13.0	0.3	5.4	1	–12.47	–12.01	3.91	4.95
FT Eq VTA/07 7	VTA V6	51–27	P3/4	53.0	38.0	71.70	–11.6	0.06	–8.4	0.08	22.3	13.4	0.3	4.6	1	–11.95	–11.57	5.10	5.96
FT Eq VTA/7 1	VTA V6	51–27	P/M	23.0	–	–	–9.2	0.14	–4.8	0.11	26.0	12.4	0.3	1.7	2	–13.25	–12.68	2.14	3.44
FT Eq VTA/07 5	VTA V14	51–27	M3	60.0	–	–	–11.6	0.07	–9.1	0.05	21.5	12.8	0.3	4.8	1	–12.73	–12.23	3.32	4.45
FT Eq VTA/07 8	VTA V14	51–27	P3/4	61.0	47.0	77.05	–11.0	0.14	–7.6	0.13	23.1	13.6	0.3	3.3	1	–11.69	–11.34	5.69	6.47
FT Eq BON/02 1	GC	~80	P2?	34.0	24.0	70.59	–11.7	0.06	–8.7	0.09	21.9	12.9	0.1	3.8	2	–12.60	–12.12	3.62	4.70
FT Eq BON/02 2	GC	~80	M1/2	38.0	20.0	52.63	–11.6	0.07	–8.8	0.11	21.8	11.9	0.3	5.5	2	–13.90	–13.23	0.67	2.18
<i>Coelodonta antiquitatis</i>																			
FT Rh CTD/00 3	VTA SY	51–27	M2	58.0	51.0	87.93	–11.1	0.13	–7.7	0.12	22.9	12.9	0.3	3.0	1	–	–12.12	–	4.70
FT Rh CTD/00 4	VTA SY	51–27	P2	42.0	22.0	52.38	–11.6	0.05	–8.8	0.15	21.9	13.0	0.2	5.2	2	–	–12.01	–	4.95
FT Ma VTA/7 2	VTA V14	51–27	P2	33.0	29.0	87.88	–11.3	0.06	–7.5	0.10	23.1	13.9	0.3	3.4	2	–	–11.01	–	7.23
FT Ma VTA/7 3	VTA V14	51–27	P2	32.0	21.0	65.63	–11.0	0.06	–7.5	0.09	23.2	10.9	0.3	3.5	2	–	–14.34	–	–0.34
FT Ma VTA/7 4	VTA V14	51–27	D3	23.0	–	–	–10.8	0.04	–7.2	0.06	23.4	14.5	0.3	3.6	2	–	–10.35	–	8.74
FT Ma VTA/7 5	VTA V14	51–27	M2	59.0	49.0	83.05	–11.3	0.11	–7.3	0.07	23.4	14.8	0.3	3.8	2	–	–10.01	–	9.50
FT Rh VTA/07 14	VTA V14	51–27	M3	49.0	–	–	–11.3	0.11	–7.0	0.10	23.7	13.3	0.3	4.1	1	–	–11.68	–	5.71
FT Rh BON/02 4	GC	~80	M2	56.0	44.0	78.57	–11.6	0.10	–7.3	0.09	23.4	13.1	0.2	4.9	2	–	–11.90	–	5.21
FT Rh BON/02 5	GC	~80	M2	56.0	36.0	64.29	–11.3	0.10	–6.6	0.09	24.1	14.5	0.2	4.5	2	–	–10.35	–	8.74
FT Rh BON/02 6	GC	~80	P4?	46.0	41.0	89.13	–11.6	0.09	–7.8	0.12	22.9	14.2	0.0	7.5	2	–	–10.68	–	7.98
FT Rh BON/02 7	GC	~80	M	41.0	23.0	56.10	–11.3	0.09	–6.9	0.09	23.7	13.0	0.1	6.6	2	–	–12.01	–	4.95
<i>Bison priscus</i>																			
FT Ma VTA/6 5	VTA V1	51–27	M1	14.0	11.0	78.57	–14.5	0.04	–8.3	0.08	22.3	13.4	0.3	3.6	2	–11.39	–11.57	6.37	5.96
FT Bi VTA/06 2	VTA V2	51–27	–	37.0	22.0	59.46	–11.0	0.08	–6.1	0.11	24.6	14.5	0.6	5.7	2	–10.09	–10.35	9.32	8.74
FT Ma VTA/6 6	VTA V2	51–27	M2/3	35.0	21.0	60.00	–10.8	0.05	–6.5	0.09	24.2	15.7	0.3	5.8	2	–8.67	–9.01	12.54	11.77
FT Bi VTA/07 12	VTA V6	51–27	m2	46.0	39.0	84.78	–10.1	0.08	–8.0	0.09	22.7	13.4	0.3	4.4	1	–11.39	–11.57	6.37	5.96
FT Bi VTA/07 13	VTA V6	51–27	m2	52.0	45.0	86.54	–10.4	0.11	–8.3	0.14	22.4	13.2	0.3	4.1	1	–11.62	–11.79	5.83	5.46
FT Ma VTA/7 7	VTA V6	51–27	M2	48.0	31.0	64.58	–10.8	0.07	–7.7	0.09	23.0	14.0	0.3	4.0	2	–10.68	–10.90	7.98	7.48
FT Ma VTA/7 8	VTA V6	51–27	M2/3	49.0	32.0	65.31	–12.4	0.04	–6.6	0.08	24.1	16.3	0.3	5.6	2	–7.97	–8.35	14.15	13.28
FT Bi BON/02 3	GC	~80	M1/2	11.0	9.0	81.82	–10.5	0.08	–8.1	0.06	22.5	14.8	0.3	5.9	2	–9.74	–10.01	10.12	9.50

**Table 4**  
Mean carbon ( $\delta^{13}\text{C}$ ) and oxygen ( $\delta^{18}\text{O}_{\text{CO}_3}$  and  $\delta^{18}\text{O}_{\text{PO}_4}$ ) isotopic values of the analysed tooth enamel from the megaherbivores of Boncourt-Grand Combe (GC) and Courtedoux-Vâ Tche Tchâ (VTA), along with the mean calculated  $\delta^{18}\text{O}_{\text{H}_2\text{O}}$  values and paleotemperatures.  $T$  ( $^{\circ}\text{C}$ ) is calculated based on the general equation for mammals (Amiot et al., 2004).

Taxon	n	Dolines	Age (ka)	$\delta^{13}\text{C}_{\text{VPDB}}$ (‰)	$\sigma$	$\delta^{18}\text{O}_{\text{CO}_3}$ VPDB (‰)	$\sigma$	$\delta^{18}\text{O}_{\text{CO}_3}$ VSMOW (‰)	$\sigma$	$\delta^{18}\text{O}_{\text{PO}_4}$ VSMOW (‰)	$\sigma$	$\delta^{18}\text{O}_{\text{H}_2\text{O}}$ (‰)	$\sigma$	$T$ ( $^{\circ}\text{C}$ )	$\sigma$	
<i>Mammuthus primigenius</i>	1	GC	~80	-12.60	-	-7.10	-	23.60	14.70	-9.15	-	11.46	-	9.24	-	
	9	VTA SY, V2, V4	51–27	-12.12	0.44	-8.07	0.88	22.60	13.63	0.88	-10.28	0.93	8.88	2.12	6.55	2.21
<i>Equis germanicus</i>	2	GC	-80	-11.65	0.07	-8.75	0.07	21.85	12.40	0.71	-13.25	0.92	2.14	2.09	3.44	1.78
	15	VTA SY, V2, V3, V6, V14	51–27	-11.67	0.91	-7.97	1.19	22.69	13.17	0.86	-12.25	1.12	4.41	2.55	5.38	2.18
<i>Coelodonta antiquitatis</i>	4	GC	-80	-11.45	0.17	-7.15	0.52	23.53	13.70	0.76	-11.23	0.85	-	-	6.72	1.92
	7	VTA SY, V14	51–27	-11.20	0.26	-7.57	0.59	23.09	13.33	1.29	-11.65	1.44	-	-	5.78	3.27
<i>Bison priscus</i>	1	GC	-80	-10.50	-	-8.10	-	22.50	14.80	-	-9.74	-	10.12	-	9.50	-
	7	VTA V1, V2, V6	51–27	-11.43	1.54	-7.36	0.93	23.33	14.36	1.22	-10.26	1.44	8.94	3.27	8.38	3.07

fermenters (13.3%) raised on an isotopically similar diet (Passey et al., 2005). If the fractionation factor of cows also applies to bison, their teeth should have slightly higher enamel  $\delta^{13}\text{C}$  values than those of the sympatric hindgut fermenters, if they fed on plants with similar carbon isotopic composition. Bison are hypergrazers (Hoppe, 2006), and the enamel  $\delta^{13}\text{C}$  values indicate that they fed on  $\text{C}_3$  grasses with  $\delta^{13}\text{C}$  values of around  $-25.5\text{\textperthousand}$  in Ajoie. This is in agreement with the fact that  $\text{C}_4$  grasses never reached Central and Northern Europe due to climatic and ecological reasons (e.g., Cerling et al., 1997). The other taxa were also predominantly grazers, and even though their tooth enamel displays lower  $\delta^{13}\text{C}$  values than bison, they ingested plants with similar or slightly higher  $\delta^{13}\text{C}$  values of around  $-25.5$  to  $-24.5\text{\textperthousand}$ , applying the bioapatite-diet isotope enrichment of 13.3% for extant large hindgut fermenters (Passey et al., 2005).

*Mammuthus primigenius* particularly shows the lowest mean  $\delta^{13}\text{C}$  value of all taxa, despite its similar digestive physiology and diet as those of woolly rhinoceroses and horses (hindgut fermenters). According to different studies on mammoth's stomach contents, tree barks and twigs probably constituted a small but significant part of their winter diet (e.g., Vereschagin and Baryshnikov, 1982; Van Geel et al., 2008, 2010). Such lignin rich plant parts have lower  $\delta^{13}\text{C}$  values and may explain the low mean enamel value of the mammoths, even though they predominantly ate grasses and herbs.

#### Oxygen isotopic composition ( $\delta^{18}\text{O}_{\text{PO}_4}$ )

In both time periods (GC and VTA), the megaherbivore teeth display similar mean  $\delta^{18}\text{O}_{\text{PO}_4}$  values of around 13.5‰ with a total range of 3‰ and 5‰, respectively (Fig. 3B and D; Table 3). Such a variability is not unusual for terrestrial mammals, it may be explained by the variability of water sources (e.g., due to animal migration, seasonality of meteoric water  $\delta^{18}\text{O}$  values, intake from food plants; Clementz et al., 2006). Additional time averaging in the doline infillings, comprising mammal remains from different climatic phases might have contributed to the variability of  $\delta^{18}\text{O}_{\text{PO}_4}$  values.

Terrestrial paleoclimatic reconstructions based on  $\delta^{18}\text{O}_{\text{PO}_4}$  values have been attempted by many studies (e.g., Longinelli, 1984; Sharp and Cerling, 1998; Tütken et al., 2007; García-Alix et al., 2012). Assuming that similar water sources were ingested by animals of the same species in the same area, then the precipitation of apatite in teeth and bones should have occurred under the same conditions, and there is thus a linear relationship between the  $\delta^{18}\text{O}$  values recorded in tooth enamel and those of the meteoric water ( $\delta^{18}\text{O}_{\text{H}_2\text{O}}$ ; Longinelli, 1984). In turn, the  $\delta^{18}\text{O}_{\text{H}_2\text{O}}$  values are related with temperature and precipitation (e.g., Luz et al., 1990; Ayliffe et al., 1992). The  $\delta^{18}\text{O}_{\text{H}_2\text{O}}$  values were calculated from the  $\delta^{18}\text{O}_{\text{PO}_4}$  values using species-specific calibrations established for modern taxa of the studied extinct mammals, assuming that the modern analogues have similar metabolism and isotopic fractionation to the extinct ones (Eq. (1) for elephants, Ayliffe et al., 1992; Eq. (2) for horses, Delgado Huertas et al., 1995; Eq. (3) for bison, Hoppe, 2006). Only for *C. antiquitatis*, the general equation for mammals was used (Eq. (4), Amiot et al., 2004), as no species-specific equation is available yet.

$$\text{Elephant}, \delta^{18}\text{O}_{\text{H}_2\text{O}} = 1.06 \times \delta^{18}\text{O}_{\text{PO}_4} - 24.78. \quad (1)$$

$$\text{Equus}, \delta^{18}\text{O}_{\text{H}_2\text{O}} = 1.30 \times \delta^{18}\text{O}_{\text{PO}_4} - 29.35. \quad (2)$$

$$\text{Bison}, \delta^{18}\text{O}_{\text{H}_2\text{O}} = 1.18 \times \delta^{18}\text{O}_{\text{PO}_4} - 27.2. \quad (3)$$

$$\text{All mammals}, \delta^{18}\text{O}_{\text{H}_2\text{O}} = 1.11 \times \delta^{18}\text{O}_{\text{PO}_4} - 26.44. \quad (4)$$

In turn, the mean annual air temperature (MAT) can be estimated according to a relation established for Switzerland between present-

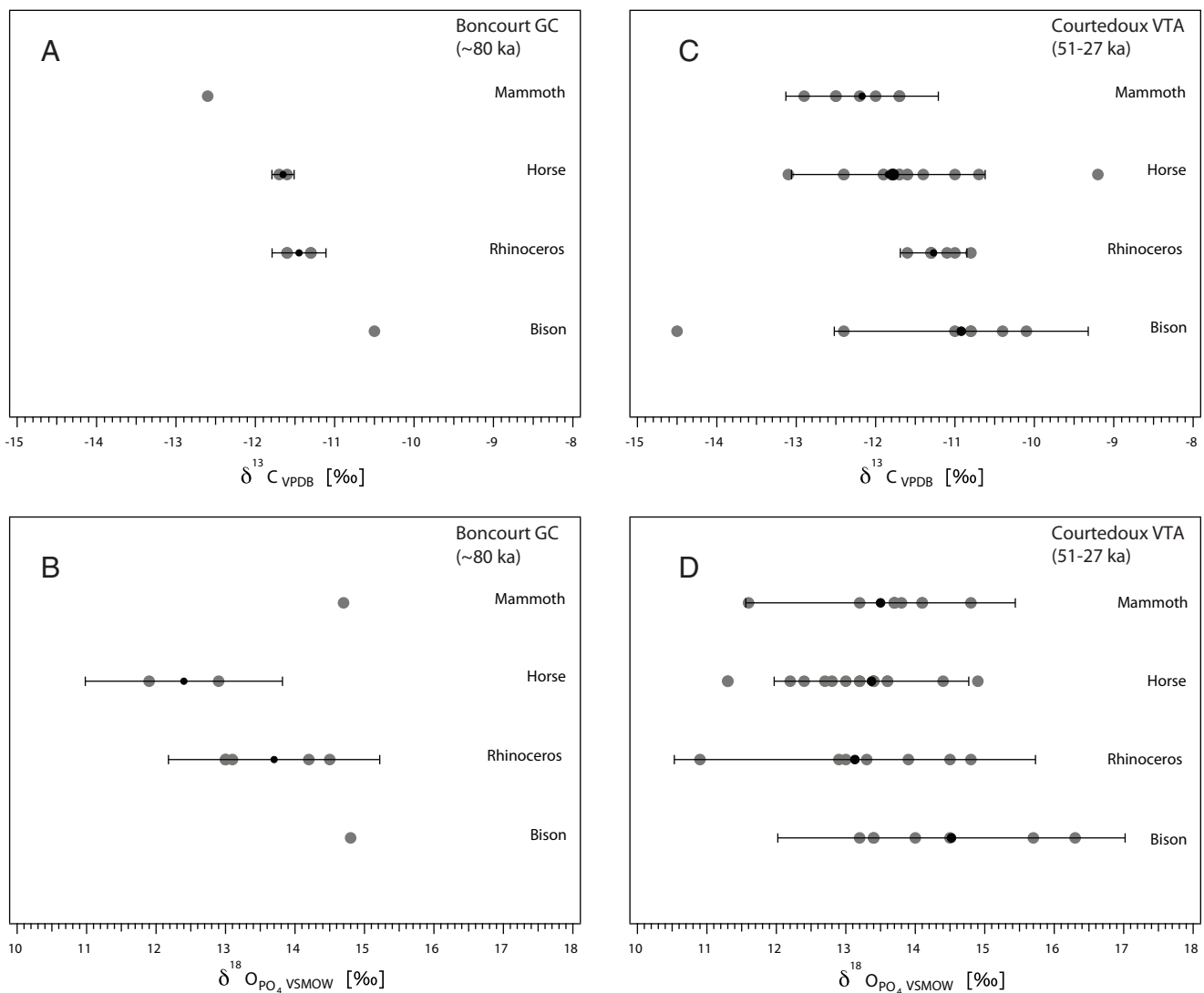


**Figure 3.** Carbon ( $\delta^{13}\text{C}$ ) and oxygen ( $\delta^{18}\text{O}_{\text{PO}_4}$ ) isotopic compositions of tooth enamel of the megaherbivores [*Mammuthus primigenius* (mammoth), *Equus germanicus* (horse), *Coelodonta antiquitatis* (rhinoceros), *Bison priscus* (bison)] from Ajoie. A and B, results from the doline of Boncourt-Grand Combe; C and D, results from the dolines of Courtedoux-Vâ Tche Tchâ. Smaller black symbols and error bars: mean and standard deviation for each species. Anatomical determinations of the teeth according to Rothen et al. (2011), Savoy et al. (2012), and DB and LS (pers. obs.).

day precipitation  $\delta^{18}\text{O}_{\text{H}_2\text{O}}$  values and air temperature (Eq. (5); Tütken et al., 2007):

$$\text{MAT}[\text{°C}] = (\delta^{18}\text{O}_{\text{H}_2\text{O}} + 14.19) \div 0.44. \quad (5)$$

As stated by Tütken et al. (2007), the  $\delta^{18}\text{O}_{\text{H}_2\text{O}}$  values of *M. primigenius* are a reliable proxy for estimating paleotemperatures, as large, obligate drinking mammals with low metabolism reflect environmental values accurately (e.g., Bryant and Froelich, 1995). The mean  $\delta^{18}\text{O}_{\text{H}_2\text{O}}$  values obtained for mammoths in VTA and the related MAT average  $-10.3 \pm 0.9\%$  and  $8.9 \pm 2.1\text{°C}$ , respectively. In turn, the MAT calculated with the whole dataset, including the four mammalian species, ranges from  $4.4 \pm 2.6\text{°C}$  (lowest mean value from *E. germanicus*) to  $8.9 \pm 3.3\text{°C}$  (highest mean values from *B. priscus*), and yields an average MAT of  $6.5 \pm 3.3\text{°C}$  for all mammals. The paleotemperatures calculated with the general equation for mammals (Eq. (4): Amiot et al., 2004; columns \* and \*\* of Table 3 and column T(°C)\* of Table 4) give a mean value of  $6.3 \pm 2.7\text{°C}$ , which is consistent with that obtained with species-specific calibrations (Tables 3 and 4). The average paleotemperature of VTA is similar to that estimated from the mammal

assemblage of the older doline of GC, averaging  $6.6 \pm 3.6\text{°C}$  (compared to a value of  $6.5 \pm 2.7\text{°C}$  if general equation for mammals is used). Hence, during MIS5a (~80 ka) and MIS3 (~45 to 35 ka), similar MAT around  $6.5\text{°C}$  prevailed in the Ajoie region.

#### The Ajoie region in the European climatic context during MIS5a and 3

The continuous pollen sequence for the last 140 ka of the Grande Pile peat bog (Vosges, NE France) recorded relative temperate climatic conditions at around 80 ka, corresponding to a latest Early Glacial interstadial, so-called Saint-Germain II (Woillard, 1978). According to De Beaulieu and Reille (1992) and Van Vliet-Lanoë and Guillocheau (1995), the chronostratigraphy and the climatic trends of this interstadial correlate to the Odderade interstadial of Northern Europe (GI21; Blockley et al., 2012). The OSL dating of the sediments from the doline infilling of GC and the  $\delta^{18}\text{O}$  values of the associated mammals correspond well to this climatic interval and are thus in agreement with the OSL-age of the locality (~80 ka).

Figure 5 illustrates estimations of MAT reconstructed from enamel  $\delta^{18}\text{O}_{\text{PO}_4}$  values of mammal teeth from European localities dated to the late middle-late Pleistocene (from 145 to 16.5 ka), in comparison to

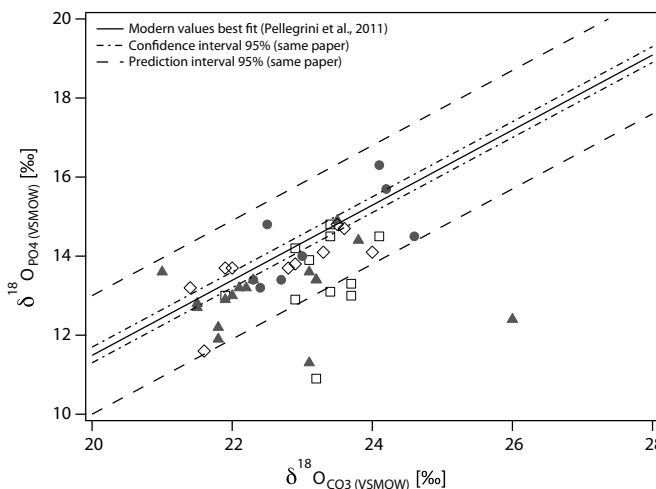


**Figure 4.** Oxygen isotope compositions of the carbonate ( $\delta^{18}\text{O}_{\text{CO}_3}$ ) and phosphate ( $\delta^{18}\text{O}_{\text{PO}_4}$ ) of the enamel apatite of all mammal teeth from the doline of Boncourt-Grand Combe and Courtedoux-Vâ Tche Tchâ. The isotopic equilibrium line between carbonate and phosphate  $\delta^{18}\text{O}$  values is plotted for reference along with the 95% confidence interval and 95% prediction interval calculated by Pellegrini et al. (2011) on modern vertebrates. White squares: *Coelodonta antiquitatis*; white diamonds: *Mammuthus primigenius*; grey circles: *Bison priscus*; grey triangles: *Equus germanicus*.

those of the doline infillings of Ajoie (Courtedoux-Vâ Tche Tchâ and Boncourt-Grand Combe; Fig. 5). According to Fabre et al. (2011), the middle and late Pleistocene cave of La Baume de Gigny (French Jura, France) recorded paleotemperatures of around  $10 \pm 2^\circ\text{C}$  at  $\sim 145$  ka (level XXI), which are similar to the  $9 \pm 3^\circ\text{C}$  obtained by Bernard et al. (2009) for the contemporaneous locality of Coudoulous I (Lot, France; Fig. 5.). Fabre et al. (2011) also observed a decrease in temperature reaching 5 to  $7^\circ\text{C}$  a few thousand years later; this drop may be contemporaneous to the older part of the site of Hallera (Poland, 115–74 ka, Fig. 5, Skrzypek et al., 2011) and to GC ( $\sim 80$  ka, Fig. 5), both of which recorded paleotemperatures between  $6.5$  and  $7^\circ\text{C}$  for MIS5a.

Paleotemperatures estimated in many European localities dated to MIS3 show large variations (MAT between  $3.5$  and  $12^\circ\text{C}$ , Fig. 5) in nearly-contemporaneous sites during this stage lasting around 30 ka. However, most of the sites during MIS3 recorded average MATs between  $3$  and  $7^\circ\text{C}$  (South Britain, Arppe and Karhu, 2010; Western Germany, Arppe and Karhu, 2010; Niederweningen, Switzerland, Tütken et al., 2007; Hallera, Poland, Skrzypek et al., 2011; Fig. 5), corresponding to the value calculated for VTA (around  $6.5 \pm 3.3^\circ\text{C}$ ; Fig. 5). The warmest paleotemperatures during MIS3 were recorded in young sites in the French Jura (Gigny,  $\sim 33$  ka, Fabre et al., 2011; Fig. 5) and in Spain (El Padul, 40–30 cal ka BP, García-Alix et al., 2012; Fig. 5) with MAT of  $12$  and  $10^\circ\text{C}$ , respectively. The large scatter of reconstructed MAT for MIS3 likely relates to sampling of mammals from different stadials or interstadials, and probably also from different geographic and topographic settings.

In their stable isotope study of the mammoths from the peat deposits of Niederweningen (NE Switzerland), Tütken et al. (2007) estimated a MAT of around  $4.3 \pm 2.1^\circ\text{C}$  during the time interval  $\sim 50$  to 45 cal ka BP, based on  $\delta^{18}\text{O}_{\text{PO}_4}$  values ranging from  $10.3$  to  $13.9\text{\textperthousand}$  (Fig. 5). This period was slightly older than the whole filling phase of the dolines of VTA and may possibly correspond to the Greenland Stadials/Interstadials 12 to 13 (Blockley et al., 2012). The mammals from VTA dolines in Ajoie probably lived under somewhat warmer climatic conditions a few thousand years later, during an interval (51–27 ka) that likely corresponds to the succession of mild/cold periods of Charbon, Stadial IV, and Grand Bois of the Grande Pile peat bog (Woillard, 1978; de Beaulieu and Reille, 1992). This time interval covers the Greenland Stadials/Interstadials 7 to 12 of the Greenland ice-core records (Blockley et al., 2012), correlated to the end of the MIS3.

The lowest paleotemperatures were recorded in mammalian bioapatite during the LGM, with sites documented in Southwest Russia (18.0–16.5 cal ka BP; Arppe and Karhu, 2010; Fig. 5) and Poland (Kraków Spadzista Street,  $\sim 24$  cal ka BP; Pryor et al., 2013; Fig. 5), with MAT values ranging between  $0.5^\circ\text{C}$  and  $1^\circ\text{C}$ , respectively. Thus, the doline records of Ajoie fit well in the picture of reconstructed MAT for the late Pleistocene of Europe. Particularly, the results obtained for VTA concur with the alternating warm and cold phases recorded during MIS3.

Finally, the mean  $\delta^{18}\text{O}_{\text{H}_2\text{O}}$  value calculated from the megaherbivore teeth of Courtedoux-Vâ Tche Tchâ (51–27 ka) fits well within the spatial distribution of oxygen isotopic composition of glacial precipitation (52 to 24 ka) reconstructed by Arppe and Karhu (2010) for Europe (Fig. 6). For the Ajoie region, enclosed northwards by the Rhine Graben and southwards by the Swiss Jura Mountains,  $\delta^{18}\text{O}_{\text{H}_2\text{O}}$  values of around  $-10\text{\textperthousand}$  were reconstructed based on large mammal teeth prior to the Last Glacial Maximum ( $\sim 45$  to 35 ka). Our results confirm the western boundary of the region recording lower mean meteoric water  $\delta^{18}\text{O}_{\text{H}_2\text{O}}$  values of  $-12\text{\textperthousand}$ , constituted by NE Switzerland, S Germany and NW Austria (Arppe and Karhu, 2010). This might also contribute to the difference with the lower values reconstructed by Tütken et al.

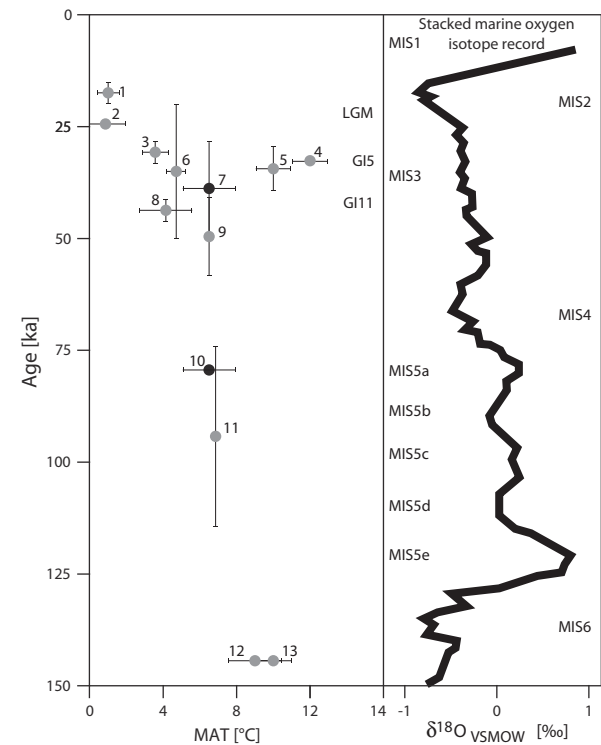


**Figure 5.** Average MAT [ $^\circ\text{C}$ ] reconstructed from enamel  $\delta^{18}\text{O}_{\text{PO}_4}$  values of fossil mammals from various European, late Pleistocene sites compared to the temperatures calculated for the dolines of Courtedoux-Vâ Tche Tchâ (6; VTA) and Boncourt-Grand Combe (9; GC). 1: Mean for Southwest Russia (18.0–16.5 cal ka BP; Arppe and Karhu, 2010); 2: Kraków Spadzista Street, Poland ( $\sim 24$  cal ka BP; Pryor et al., 2013); 3: mean for South Britain (34–32 cal ka BP; Arppe and Karhu, 2010); 4: Gigny, level VIII, France ( $\sim 33$  ka; Fabre et al., 2011); 5: El Padul, Spain (40–30 cal ka BP; García-Alix et al., 2012); 6: mean for Courtedoux-Vâ Tche Tchâ, Switzerland (51–27 ka; this study); 8: Niederweningen, Switzerland (45–40 cal ka BP; Tütken et al., 2007); 9: Hallera, Poland (59–41 ka; Skrzypek et al., 2011, including values on bones as well); 10: mean for Boncourt-Grand Combe, Switzerland ( $\sim 80$  ka; this study); 11: Hallera, Poland (115–74 ka; Skrzypek et al., 2011, including values on bones as well); 12: Coudoulous I, France ( $\sim 145$  ka; Bernard et al., 2009); 13: Gigny, level XX, France ( $\sim 145$  ka; Fabre et al., 2011). Error bars show the time spanned by each locality and the paleotemperature range (when available). Interval GI11 to 5 (glacial interstadials; Pilkington and Gibbard, 2012) is highlighted; LGM, Last Glacial Maximum; MIS, Marine Oxygen Isotope Stages; marine oxygen isotope curve and MIS according to Martinson et al. (1987).

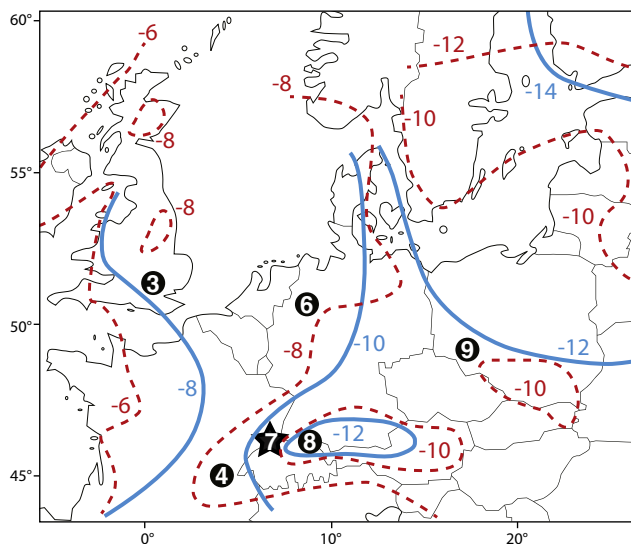


**Figure 6.** Modern (red dashed lines) and past (blue solid lines; 52–24 ka) geographic patterns of oxygen isotopic composition of precipitations according to Arppe and Karhu (2010), with new data (black star, number 7) averaging  $-10\text{\textperthousand}$  for the dolines of Courtedoux-Vâ Tche Tchâ (51–27 ka). Numbers 3, 4, 6, 7, 8 and 9 refer to MIS3 localities shown in Fig. 5 (according to Tütken et al., 2007; Arppe and Karhu, 2010; Fabre et al., 2011; Pryor et al., 2013). (For interpretation of the references to colour in this figure legend, the reader is referred to the web version of this article.)

(2007) from the slightly older ( $\sim 50$ –45 cal ka BP) mammoth teeth of Niederweningen (NW Switzerland).

## Conclusion

Stable isotope analyses of enamel from megaherbivores of the Mammoth Steppe fauna from eight  $^{14}\text{C}$ - and OSL-dated doline infillings from Boncourt-Grand Combe (GC:  $\sim 80$  ka) and Courtedoux-Vâ Tche Tchâ (VTA: 51–27 ka) yield information about the late Pleistocene climate in NW Switzerland during MIS5a and 3, respectively. Air temperatures reconstructed from mammalian enamel phosphate oxygen isotope compositions fit well within recent paleoclimatic models for the late Pleistocene, confirming previous climatic interpretations based either on ungulate mammals or on other proxies, such as rodents or pollens. Enamel  $\delta^{18}\text{O}_{\text{PO}_4}$  values of horses, bison, rhinoceroses, and mammoths indicate that these megaherbivores (from both GC and VTA) lived during mild periods of the late Pleistocene with MAT of around  $6.5^\circ\text{C}$ , only 2–3°C lower than in the Ajoie region of the Swiss Jura today.

The  $\delta^{13}\text{C}$  values of around  $-11.5\text{\textperthousand}$  indicate that these megaherbivores fed in an open  $\text{C}_3$  plant ecosystem, which is consistent with the tundra-steppe paleoenvironment reconstructed for the region by Becker et al. (2009, 2013).

## Acknowledgments

We thank the stable isotope laboratory of the University of Tübingen (Germany) for analysing the samples, the Tandem Laboratory (University of Uppsala, Sweden) for the radiocarbon dating, and the Laboratory of Geochronology (University of Köln, Germany) for the OSL dating. The Swiss Federal Roads Authority and the Office de la culture (Canton Jura, Switzerland) funded this research. LS and TT acknowledge funding by the Swiss National Science Foundation (PBFRP2-145876) and the DFG Emmy Noether Program grant TU 148/2-1 Bone Geochemistry, respectively. We thank editors C. Marean and A. Gillespie and reviewers M. Pellegrini and anonymous for improving the paper.

## References

- Amiot, R., Lécuyer, C., Buffetaut, E., Fluteau, F., Legendre, S., Martineau, F., 2004. Latitudinal temperature gradient during the Cretaceous Upper Campanian–Middle Maastrichtian:  $\delta^{18}\text{O}$  record of continental vertebrates. *Earth and Planetary Science Letters* 226, 255–272.
- Antoine, P., Rousseau, D.D., Zöller, L., Lang, A., Munaut, A.-V., Hatté, C., Fontugne, M., 2001. High-resolution record of the last interglacial-glacial cycle in the Nussloch loess-paleosol sequences, Upper Rhine Area, Germany. *Quaternary International* 76 (77), 211–229.
- Arppe, L., Karhu, J.A., 2010. Oxygen isotope values of precipitation and the thermal climate in Europe during the middle to late Weichselian ice age. *Quaternary Science Reviews* 29, 1263–1275.
- Aubry, D., Guélat, M., Detrey, J., Othenin-Girard, B., 2000. Dernier cycle glaciaire et occupations paléolithiques à Aile, Noir Bois (Jura, Suisse). Porrentruy, Office du patrimoine historique et Société jurassienne d'Emulation. Cahier d'archéologie jurassienne 10, 175.
- Ayliffe, L.K., Lister, A.M., Chivas, A.R., 1992. The preservation of glacial–interglacial climatic signatures in the oxygen isotopes of elephant skeletal phosphate. *Palaeogeography, Palaeoclimatology, Palaeoecology* 99, 179–191.
- Bassinot, F.C., Labeyrie, L.D., Vincent, E., Quidelleur, X., Shackleton, N.J., Lancelot, Y., 1994. The astronomical theory of climate and the age of the Brunhes–Matuyama magnetic reversal. *Earth and Planetary Science Letters* 126, 91–108.
- Becker, D., Aubry, D., Detrey, J., 2009. Les dolines du Pléistocène supérieur de la combe de "Vâ Tche Tchâ" (Ajoie, Suisse): un piège à reste de mammifères et artéfacts lithiques. *Quaternaire* 20, 135–148.
- Becker, D., Oppliger, J., Theuw, N., Scherler, L., Aubry, D., Braillard, L., 2013. Climat et écologie en Ajoie durant la seconde partie du Pléniglaciaire moyen weichsélien: apport des remplissages des dolines de Courtedoux-Vâ Tche Tchâ (Jura, Suisse). In: Richard, A., Schifferdecker, F., Mazimann, J.-P., Bélet-Gondat, C. (Eds.), Le peuplement de l'arc jurassien de la préhistoire au Moyen Âge. Deuxièmes Journées Archéologiques Frontalières de l'Arc Jurassien, Acte des rencontres 2007, Annales Littéraires de l'Université de Franche-Comté et Cahier d'archéologie jurassienne, Besançon-Porrentruy, pp. 13–24.
- Bernard, A., Daux, V., Lécuyer, C., Brugal, J.-P., Genty, D., Wainer, K., Gardien, V., Fourel, F., Jaubert, J., 2009. Pleistocene seasonal temperature variations recorded in the  $\delta^{18}\text{O}$  of *Bison priscus* teeth. *Earth and Planetary Science Letters* 283, 133–143.
- Blockley, S.P.E., Lane, C.S., Hardiman, M., Rasmussen, S.O., Seierstad, I.K., Steffensen, J.P., Svensson, A., Lotter, A.F., Turney, Chris S., Ramsey, C.B., 2012. Synchronisation of palaeoenvironmental records over the last 60,000 years, and an extended INTIMATE1 event stratigraphy to 48,000 b2k. *Quaternary Science Reviews* 36, 2–10.
- Braillard, L., 2006. Rôle de la tectonique et de la stratigraphie dans la formation des vallées sèches de l'Ajoie (JU-Suisse). *Geofocus* 14, 224.
- Braillard, L., 2009. Remplissages quaternaires et paléohydrologie des vallées sèches d'Ajoie (Jura tabulaire, Suisse). *Geographica Helvetica* 64 (3), 148–156.
- Brugal, J.-P., Croitor, R., 2007. Evolution, ecology and biochronology of herbivore associations in Europe during the last 3 million years. *Quaternaire* 18, 129–152.
- Bryant, J.D., Froelich, P.N., 1995. A model of oxygen isotope fractionation in body water of large mammals. *Geochimica et Cosmochimica Acta* 59, 4523–4537.
- Bryant, J.D., Froelich, P.N., Showers, W.J., Genna, B.J., 1996. Biologic and climatic signals in the oxygen isotopic composition of Eocene–Oligocene equid enamel phosphate. *Palaeogeography, Palaeoclimatology, Palaeoecology* 126, 75–89.
- Cerling, T.E., Harris, J.M., 1999. Carbon isotope fractionation between diet and bioapatite in ungulate mammals and implications for ecological and palaeoecological studies. *Oecologia* 120, 347–363.
- Cerling, T.E., Harris, J.M., MacFadden, B.J., Leaky, M.G., Quade, J., Eisenmann, V., Ehleringer, J.R., 1997. Global vegetation change through the Miocene–Pliocene boundary. *Nature* 389, 153–158.
- Cerling, T.E., Hart, J.A., Hart, T.B., 2004. Stable isotope ecology in the Ituri Forest. *Oecologia* 138, 5–12.
- Clementz, M.T., Goswami, A., Gingerich, P.D., Koch, P.L., 2006. Isotopic records from early whales and sea cows: contrasting patterns of ecological transition. *Journal of Vertebrate Paleontology* 26, 355–370.
- Coplen, T.B., Kendall, C., Hopple, J., 1983. Comparison of stable isotope reference samples. *Nature* 302, 236–238.
- Dansgaard, W., 1964. Stable isotopes in precipitation. *Tellus* 16, 436–468.
- De Beaulieu, J.-L., Reille, M., 1992. The last climatic cycle at La Grande Pile (Vosges, France) – a new pollen profile. *Quaternary Science Reviews* 11, 431–438.
- Delgado Huertas, A., Iacumin, P., Stenni, B., Chillón, S., Longinelli, A., 1995. Oxygen isotope variations of phosphate in mammalian bone and tooth enamel. *Geochimica et Cosmochimica Acta* 59, 4299–4305.
- Diefendorf, A.F., Mueller, K.E., Wing, S.L., Koch, P.L., Freeman, K.H., 2010. Global patterns in leaf  $^{13}\text{C}$  discrimination and implications for studies of past and future climate. *Proceedings of the National Academy of Sciences* 107, 5738–5743.
- Fabre, M., Lécuyer, C., Brugal, J.-P., Amiot, R., Fourel, F., Martineau, F., 2011. Late Pleistocene climatic change in the French Jura (Gigny) recorded in the  $\delta^{18}\text{O}$  of phosphate from ungulate tooth enamel. *Quaternary Research* 85, 605–613.
- Farquhar, G.D., Ehleringer, J.R., Hubrick, K.T., 1989. Carbon isotopic discrimination and photosynthesis. *Annual Reviews of Plant Physiology and Molecular Biology* 40, 503–537.
- Feranec, R.S., 2007. Stable carbon isotope values reveal evidence of resource partitioning among ungulates from modern  $\text{C}_3$ -dominated ecosystems in North America. *Palaeogeography, Palaeoclimatology, Palaeoecology* 252, 575–585.
- Feranec, R.S., MacFadden, B.J., 2006. Isotopic discrimination of resource partitioning among ungulates in  $\text{C}_3$ -dominated communities from the Miocene of Florida and California. *Paleobiology* 32, 191–205.

- Fricke, H.C., O'Neil, J.R., 1996. Inter- and intra-tooth variation in the oxygen isotope composition of mammalian tooth enamel phosphate: implications for palaeoclimatological and palaeobiological research. *Palaeogeography, Palaeoclimatology, Palaeoecology* 126, 91–99.
- Fricke, H.C., O'Neil, J.R., 1999. The correlation between  $^{18}\text{O}/^{16}\text{O}$  ratios of meteoric water and surface temperature: its use in investigating terrestrial climate change over geologic time. *Earth and Planetary Science Letters* 170, 181–196.
- Fricke, H.C., Clyde, W.C., O'Neil, J.R., 1998. Intra-tooth variations in  $\delta^{18}\text{O}_{\text{PO}_4}$  of mammalian tooth enamel as a record of seasonal variations in continental climate variables. *Geochimica et Cosmochimica Acta* 62, 1839–1850.
- García-Alix, A., Delgado Huertas, A., Martín Suárez, E., 2012. Unravelling the Late Pleistocene habitat of the southernmost woolly mammoths in Europe. *Quaternary Science Reviews* 32, 75–85.
- Guélat, M., 2005. Le Quaternaire dans le canton du Jura. *Actes de la Société jurassienne d'Émulation* 108, 9–31.
- Gygi, R., 2000. Integrated stratigraphy of the Oxfordian and Kimmeridgian (Late Jurassic) in northern Switzerland and adjacent southern Germany. *Denkschriften der Schweizerischen Akademie der Naturwissenschaften* 104, 1–151.
- Haq, B.U. (Ed.), 2007. *The Geological Time Scale*, Sixth edition (Wall Chart). Elsevier.
- Heaton, T.H.E., 1999. Spatial, species, and temporal variations in the  $^{13}\text{C}/^{12}\text{C}$  ratios of  $\text{C}_3$  plants: implications for paleodiet studies. *Journal of Archaeological Science* 26, 637–649.
- Hoppe, K.A., 2006. Correlation between the oxygen isotope ratio of North American bison teeth and local waters: implications for paleoclimatic reconstructions. *Earth and Planetary Sciences Letters* 244, 408–417.
- Johnsen, S.J., Clausen, H.B., Dansgaard, W., Gundestrup, N.S., Hammer, C.U., Andersen, U., Andersen, K.K., Hvidberg, C.S., Dahl-Jensen, D., Steffensen, J.P., Shoji, H., Sveinbjörnsdóttir, A.E., White, J., Jouzel, J., Fisher, D., 1997. The  $\delta^{18}\text{O}$  record along the Greenland Ice-core Project deep ice core and the problem of possible Eemian climatic instability. *Journal of Geophysical Research* 102, 26397–26410.
- Johnson, C.N., 2002. Determinants of loss of mammal species during the Late Quaternary "megafauna" extinctions: life history and ecology, but not body size. *Proceedings of the Royal Society B* 269, 2221–2227.
- Kahlke, R.-D., 1999. *The History of the Origin, Evolution and Dispersal of the Late Pleistocene *Mammuthus*–*Coolodontia* Faunal Complex in Eurasia (Large Mammals)*. Mammoth Site of Hot Springs, Rapid City, (219 pp.).
- Koch, P.L., 1998. Isotopic reconstruction of past continental environments. *Annual Review of Earth and Planetary Sciences* 26, 573–613.
- Koch, P.L., 2007. Isotopic study of the biology of modern and fossil vertebrates. In: Michener, R., Lajtha, K. (Eds.), *Stable Isotopes in Ecology and Environmental Science*. Blackwell, Oxford, pp. 99–154.
- Koch, P.L., Tuross, N., Fogel, M.L., 1997. The effects of sample treatment and diagenesis on the isotopic integrity of carbonate in biogenic hydroxyapatite. *Journal of Archaeological Science* 24, 417–429.
- Kohn, M.J., 1996. Predicting animal  $\delta^{18}\text{O}$ : accounting for diet and physiological adaptation. *Geochimica et Cosmochimica Acta* 60, 4811–4829.
- Kohn, M.J., 2010. Carbon isotope compositions of terrestrial  $\text{C}_3$  plants as indicators of (paleo)ecology and (paleo)climate. *Proceedings of the National Academy of Sciences* 107, 19691–19695.
- Kohn, M.J., Cerling, T.E., 2002. Stable isotope compositions of biological apatite. In: Kohn, M.J., Rakovan, J., Hughes, J.M. (Eds.), *Reviews in Mineralogy and Geochemistry*, 48, pp. 455–488.
- Levin, N.E., Cerling, T.E., Passey, B.H., Harris, J.M., Ehleringer, J.R., 2006. A stable isotope aridity index for terrestrial environments. *Proceedings of the National Academy of Sciences* 103, 11201–11205.
- Longinelli, A., 1984. Oxygen isotopes in mammal bone phosphate: a new tool for paleohydrological and paleoclimatological research? *Geochimica et Cosmochimica Acta* 48, 385–390.
- Luz, B., Cormie, A.B., Schwarz, H.P., 1990. Oxygen isotope variations in phosphate of deer bones. *Geochimica et Cosmochimica Acta* 54, 1723–1728.
- Manzi, G., 2011. Before the emergence of *Homo sapiens*: overview on the Early-to-Middle Pleistocene fossil record (with a proposal about *Homo heidelbergensis* at the subspecific level). *International Journal of Evolutionary Biology*. <http://dx.doi.org/10.4061/2011/582678> (11 pp.).
- Markova, A.K., Puzachenko, A.Y., Van Kolfschoten, T., 2009. The North Eurasian mammal assemblages during the end of MIS3 (Brianskian–Late Karginian–Denekamp Interstadial). *Quaternary International* 212, 149–158.
- Martinson, D.G., Pisias, N.G., Hays, J.D., Imbrie, J., Moore Jr., T.C., Shackleton, N.J., 1987. Age dating and the orbital theory of the ice ages: development of a high-resolution 0 to 300 000-year chronostratigraphy. *Quaternary Research* 27, 1–29.
- Mellars, P., 2004. Neanderthals and the modern human colonization of Europe. *Nature* 432, 461–465.
- O'Leary, M.H., 1988. Carbon isotopes in photosynthesis. *BioScience* 38, 328–336.
- Oppliger, J., Becker, D., 2010. Morphometrical analyses of northern Birch Mice (*Sicista betulina* Pallas, 1779; Mammalia; Rodentia) discovered in a rich locality from the Late Pleistocene of Northwestern Switzerland. *Comptes Rendus Palevol* 9, 113–120.
- Passey, B.J., Robinson, T.F., Ayliffe, L.K., Cerling, T.E., Sponheimer, M., Dearing, M.D., Roeder, B.L., Ehleringer, J.R., 2005. Carbon isotope fractionation between diet, breath  $\text{CO}_2$ , and biapatite in different mammals. *Journal of Archaeological Science* 32, 1459–1470.
- Pellegrini, M., Lee-Thorp, J.A., Donahue, R.E., 2011. Exploring the variation of the  $\delta^{18}\text{O}_{\text{P}}$  and  $\delta^{18}\text{O}_{\text{c}}$  relationship in enamel increments. *Geochimica et Cosmochimica Acta* 75, 71–83.
- Pillans, B., Gibbard, P., 2012. The Quaternary period. In: Gradstein, F.M., Ogg, J.G., Schmitz, M.D., Ogg, G.M. (Eds.), *The Geologic Time Scale 2012*. Elsevier Publishing Company, pp. 979–1010.
- Pryor, A.J.E., O'Connell, T.C., Wojtal, P., Krzeminska, A., Stevens, R.E., 2013. Investigating climate at the Upper Palaeolithic site of Kraków Spadzista Street (B), Poland, using oxygen isotopes. *Quaternary International* 294, 108–119.
- Rothen, J., Becker, D., Berger, J.-P., 2011. Morphométrie des dents jugales du mammouth laineux (*Mammuthus primigenius*) découverte dans les remplissages pléistocènes de dolines d'Ajoie (Jura, Suisse). *Actes de la Société jurassienne d'émulation* 2012, 17–36.
- Rozanski, K., Araguás-Araguás, L., Confrontini, R., 1993. Isotopic patterns in modern global precipitation. In: Swart, P.K., Lohmann, K.C., McKenzie, J., Savin, S. (Eds.), *Climate Change in Continental Isotopic Records*. Geophysical Monograph, 78, pp. 1–36.
- Savoy, J., Scherler, L., Becker, D., 2012. Variabilité morphologique et biométrique des dents d'*Equus germanicus* des dolines pléistocènes d'Ajoie (Jura, Suisse). *Actes de la Société jurassienne d'émulation* 2012, 17–36.
- Sharp, W.B., Cerling, T.E., 1998. Fossil isotope records of seasonal climate and ecology: straight from the horse's mouth. *Geology* 26, 219–222.
- Skrzypek, G., Wisniewski, A., Grierson, P.F., 2011. How cold was it for Neanderthals moving to Central Europe during warm phases of the last glaciation? *Quaternary Science Reviews* 30, 481–487.
- Svensson, A., Andersson, K.K., Bigler, M., Clausen, H.B., Dahl-Jensen, D., Davies, S.M., Johnsen, S.J., Muscheler, R., Rasmussen, S.O., Röthlisberger, R., Steffensen, J.P., Vinther, B.M., 2006. The Greenland Ice Core Chronology 2005, 15–42 ka. Part 2: comparison to other records. *Quaternary Science Reviews* 25, 3258–3267.
- Tütken, T., Vennemann, T.W., 2009. Stable isotope ecology of Miocene large mammals from Sandelzhausen, southern Germany. *Paläontologische Zeitschrift* 83, 207–226.
- Tütken, T., Vennemann, T.W., Janz, H., Heizmann, E.P.J., 2006. Palaeoenvironment and palaeoclimate of the Middle Miocene lake in the Steinheim basin, SW Germany: a reconstruction from C, O, and Sr isotopes of fossil remains. *Geochimica et Cosmochimica Acta* 74, 457–491.
- Tütken, T., Furrer, H., Vennemann, T.W., 2007. Stable isotope compositions of mammoth teeth from Niederdweningen, Switzerland: implications for the Late Pleistocene climate, environment, and diet. *Quaternary International* 164–165, 139–150.
- Van Andel, T.H., Davies, W. (Eds.), 2003. *Neanderthals and Modern Humans in the European Landscape during the Last Glaciation*. McDonald Institute monographs, Cambridge.
- Van der Merwe, N.J., Medina, E., 1991. The canopy effect, carbon isotope ratios and foodwebs in Amazonia. *Journal of Archaeological Science* 18, 249–259.
- Van Geel, B., Aptroot, A., Baitinger, C., Birks, H.H., Bull, I.D., Cross, H.B., Evershed, R.P., Gravendeel, B., Kompanje, E.J.O., Kuperus, P., Mol, D., Nierop, K.G.J., Pals, J.P., Tikhonov, A.N., Van Reenen, G., Van Tienderen, P.H., 2008. The ecological implications of a Yukatan mammoth's last meal. *Quaternary Research* 69, 361–376.
- Van Geel, B., Guthrie, R.D., Altmann, J.G., Broekens, P., Bull, I.D., Gill, F.L., Jansen, B., Nieman, A.M., Gravendeel, B., 2010. Mycological evidence of coprophagy from the feces of an Alaskan Late Glacial mammoth. *Quaternary Science Reviews* 30, 2289–2303.
- Van Meerbeeck, C.J., Renssen, H., Roche, D.M., 2009. How did marine isotope stage 3 and Last Glacial Maximum climates differ? Perspectives from equilibrium simulations. *Climate of the Past* 3, 33–51.
- Van Vliet-Lanoë, B., Guillocheau, F., 1995. Évolution de l'enregistrement pédosédimentaire depuis 150 ka en France du NO et en Belgique: biorhexistasie et bilans sédimentaires. *Comptes Rendus de l'Académie des Sciences* 320, 419–426.
- Vereschagin, N.K., Baryshnikov, G.F., 1982. Paleoecology of the mammoth fauna in the Eurasian Arctic. In: Hopkins, D.M., Matthews Jr., J.V., Schweger, C.E., Young, S.B. (Eds.), *Paleoecology of Beringia*. Academic Press, New York, pp. 267–279.
- von Koenigswald, W., 2006. Climatic changes, faunal diversity, and environment of the Neanderthals in Central and Western Europe during the middle and upper Pleistocene. *Terra Nostra* 2006 (2), 35–40.
- Woillard, G., 1978. Grande Pile peat bog: a continuous pollen record for the last 140 000 yrs. *Quaternary Research* 9, 1–21.
- Zachos, J., Pagani, M., Sloan, L., Thomas, E., Billups, K., 2001. Trends, rhythms, and aberrations in global climate 65 Ma to present. *Science* 292, 686–693.